doi:10.1038/nature11674

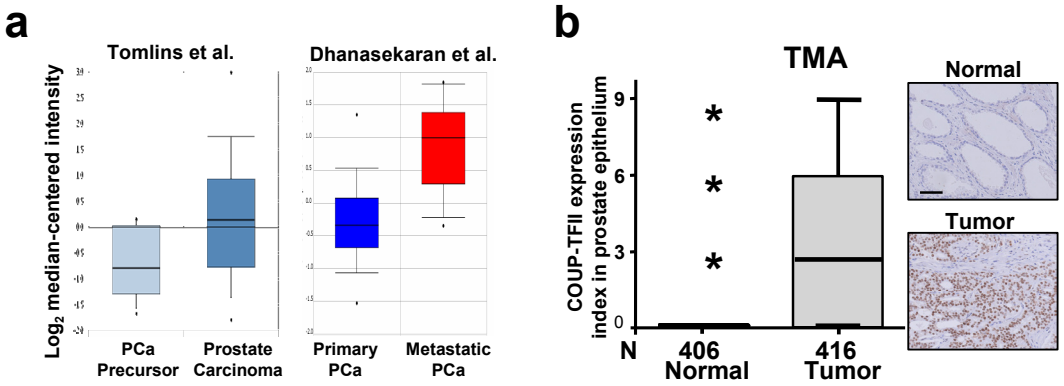

Supplementary Fig. 1. COUP-TFII expression in prostate cancer (a) Boxed plot of COUP-TFII expression levels in prostate cancer patients using Oncomine expression analysis (Dhanasekaran et al., 2001; Tomlins et al., 2007). **(b)** Wilcoxon signed-ranks test is used to calculate expression index in normal and tumor tissues. Representative COUP-TFII staining is shown on the right. N: number of patients, *: Outliers. Scale bar, 50 μm.

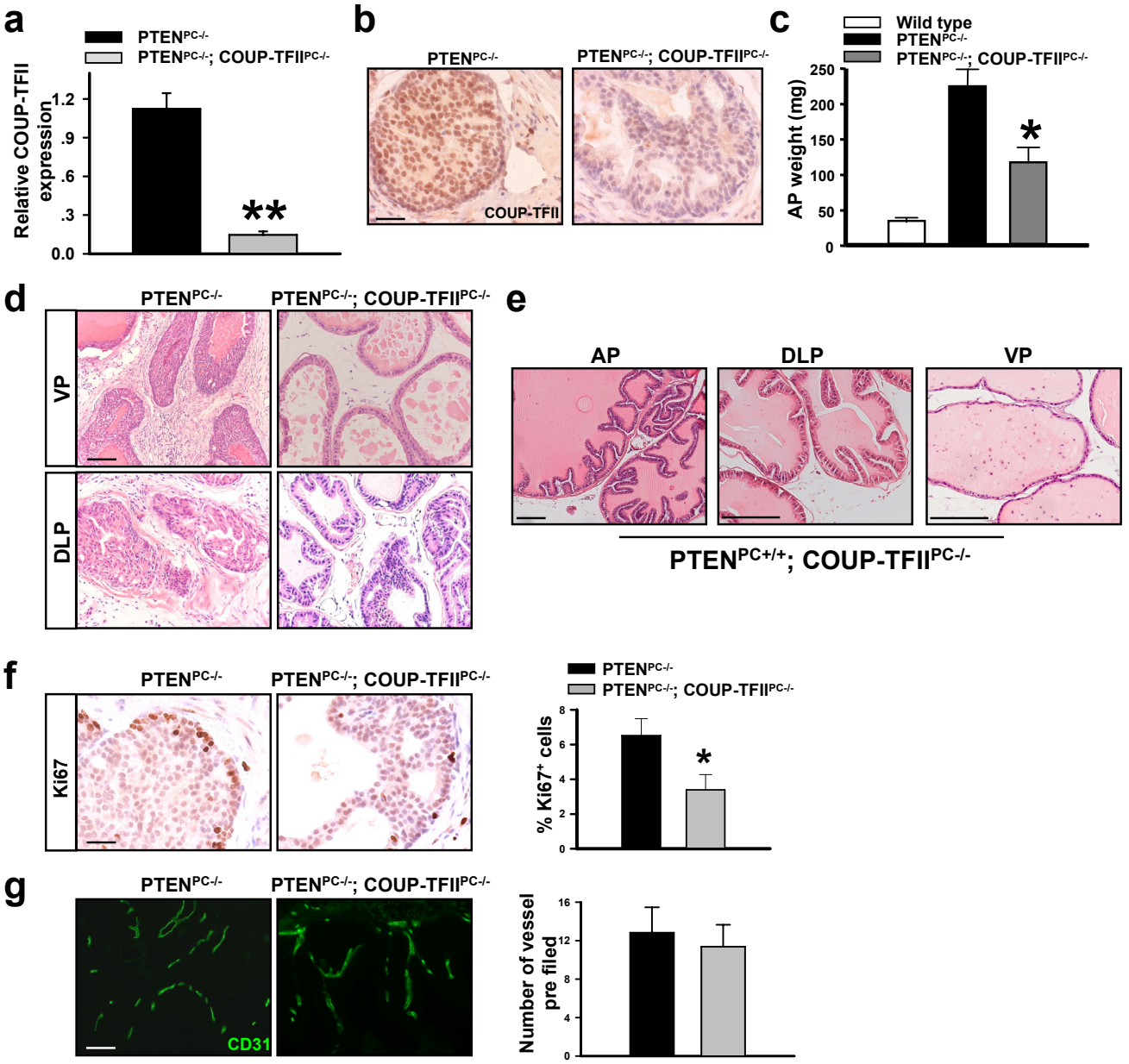

Supplementary Fig. 2. Loss of COUP-TFII inhibits prostate tumorigenesis in PTEN null mouse. (a) qRT-PCR analysis of COUP-TFII expression in prostate from PTEN$^{PC-/-}$ and PTEN$^{PC-/-}$; COUP-TFII$^{PC-/-}$ mice (N=3). **: $P < 0.01$. **(b)** Immunohistochemistry for COUP-TFII in the prostate epithelium from PTEN$^{PC-/-}$ and PTEN$^{PC-/-}$; COUP-TFII$^{PC-/-}$ mice **(c)** Anterior prostate (AP) weight of Wild type; PTEN$^{PC-/-}$ and PTEN$^{PC-/-}$; COUP-TFII$^{PC-/-}$ mice at 5 months of age (N=6). *: $P < 0.05$. **(d)** H&E staining of ventral prostate (VP) and Dorsal-lateral prostate (DLP) from PTEN$^{PC-/-}$ and PTEN$^{PC-/-}$; COUP-TFII$^{PC-/-}$ mice at 5 months of age. **(e)** H&E-stained sections of the AP, DLP and VP in COUP-TFII$^{PC-/-}$ mice. **(f)** Cell proliferation (Ki67^{+} cells) in PTEN$^{PC-/-}$ and PTEN$^{PC-/-}$; COUP-TFII$^{PC-/-}$ mice at 5 months of age (N=6). *: $P < 0.05$. **(g)** CD31 staining of prostate tumors from PTEN$^{PC-/-}$ and PTEN$^{PC-/-}$; COUP-TFII$^{PC-/-}$ mice (N=6). Scale bars in **b** and **f**, 25 μm; in **d** and **g**, 50 μm; in **e**, 100μm. Error bars, Means ± SEM.

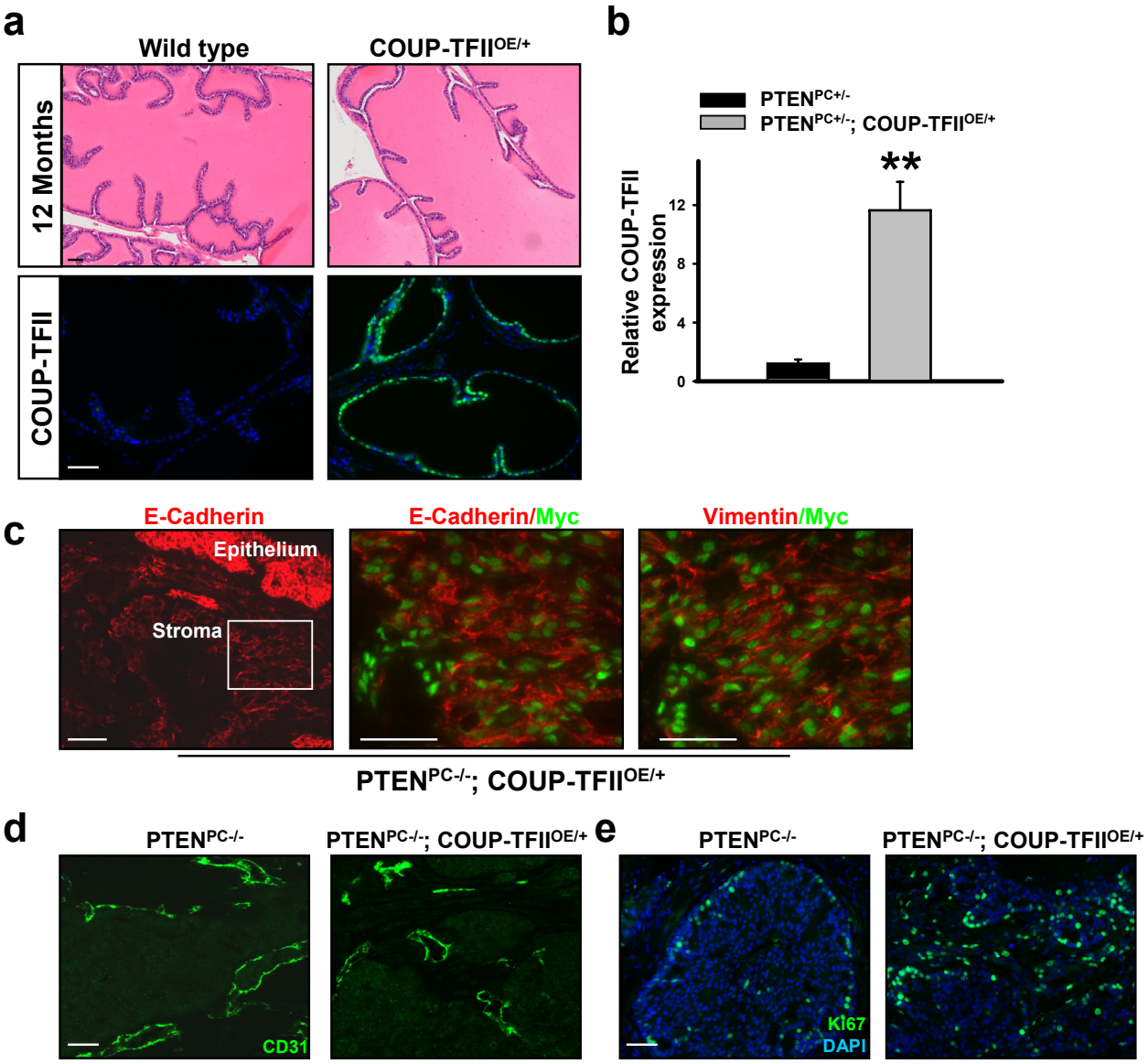

Supplementary Fig. 3. Conditional over-expression of COUP-TFII in the prostate epithelium. (a) H&E-stained sections of the AP from wild type and COUP-TFII$^{OE/+}$ mice at 12 months of age (Top); Immunohistochemical analysis of COUP-TFII expression (Bottom). **(b)** qRT-PCR analysis of COUP-TFII expression in the prostate epithelium from PTEN$^{PC+/-}$ and PTEN$^{PC+/-}$; COUP-TFII$^{OE/+}$ mice at 4 months of age (N=3). **: $P < 0.01$. **(c)** Immuostaining of E-cadherin, Myc and Vimentin expression in the invasive tumors from COUP-TFII over-expression mice at 6 months of age. Subset of the invasive tumor cells emerge undergoing epithelial-mesenchymal transition (EMT), as reflected by the reduction of E-cadherin expression as compared to the adjacent primary tumors. Since the COUP-TFII over-expression allele is fused with a Myc tag, we use Myc-positive cells to trace the epithelial origin of tumor cells and show that those invading cells are co-expressing the mesenchymal marker, Vimentin. Ki67 **(d)** and CD31 **(e)** staining of prostate tumors from PTEN $^{PC-/-}$ and PTEN$^{PC-/-}$; COUP-TFII$^{OE/+}$ mice at 6 months of age. Scale bar, 50 μm. Error bars, Means ± SEM.

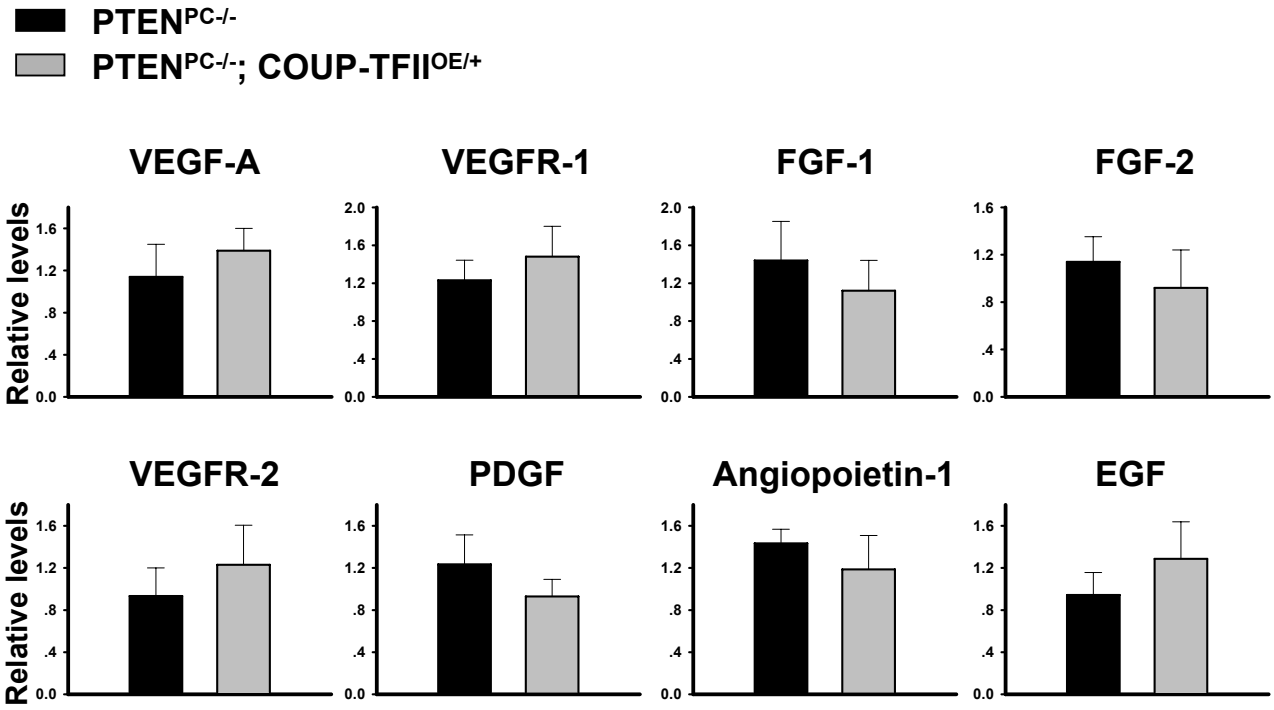

Supplementary Fig. 4. Over-expression of COUP-TFII in prostate epithelium of PTEN null mice does not affect tumor angiogenesis. qRT-PCR expression analysis of different proangiogenic factors and their primary receptors as indicated in the prostate tumors from $PTEN^{PC-/-}$ and $PTEN^{PC-/-}$; $COUP\text{-}TFII^{OE/+}$ mice. The expression of the angiogenic factors/corresponding receptors (VEGF, FGF and etc.) are not altered upon COUP-TFII over-expression (N=5). Error bars, Means ± SEM.

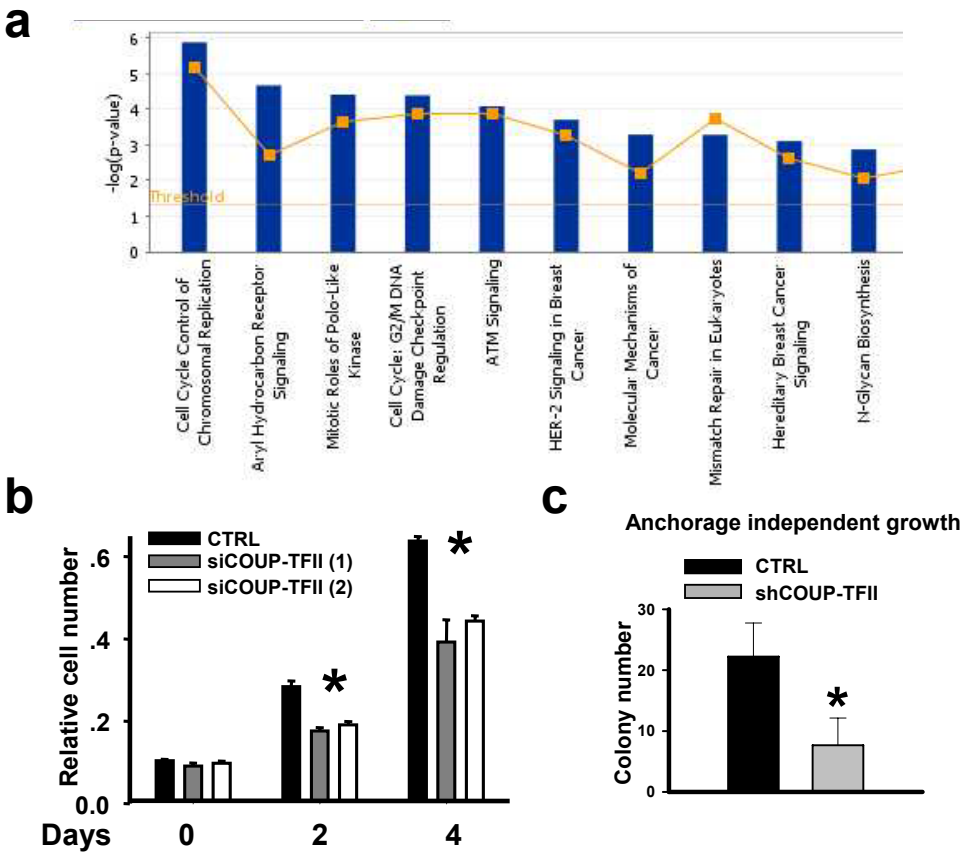

Supplementary Fig. 5. COUP-TFII is important for prostate cancer cell growth. (a) IPA analysis of COUP-TFII function in PC3 cells shows that the most significantly enriched gene-categories are related to cell growth and cell cycle progression. **(b)** *In vitro* growth of control and COUP-TFII depleted PC3 cells as measured by MTT analysis. *: $P < 0.05$. **(c)** Anchorage independent growth assay of control and COUP-TFII depleted PC3 cells. *: $P < 0.05$. The results are obtained from 3 independent repeated experiments. Error bars, Means ± SEM.

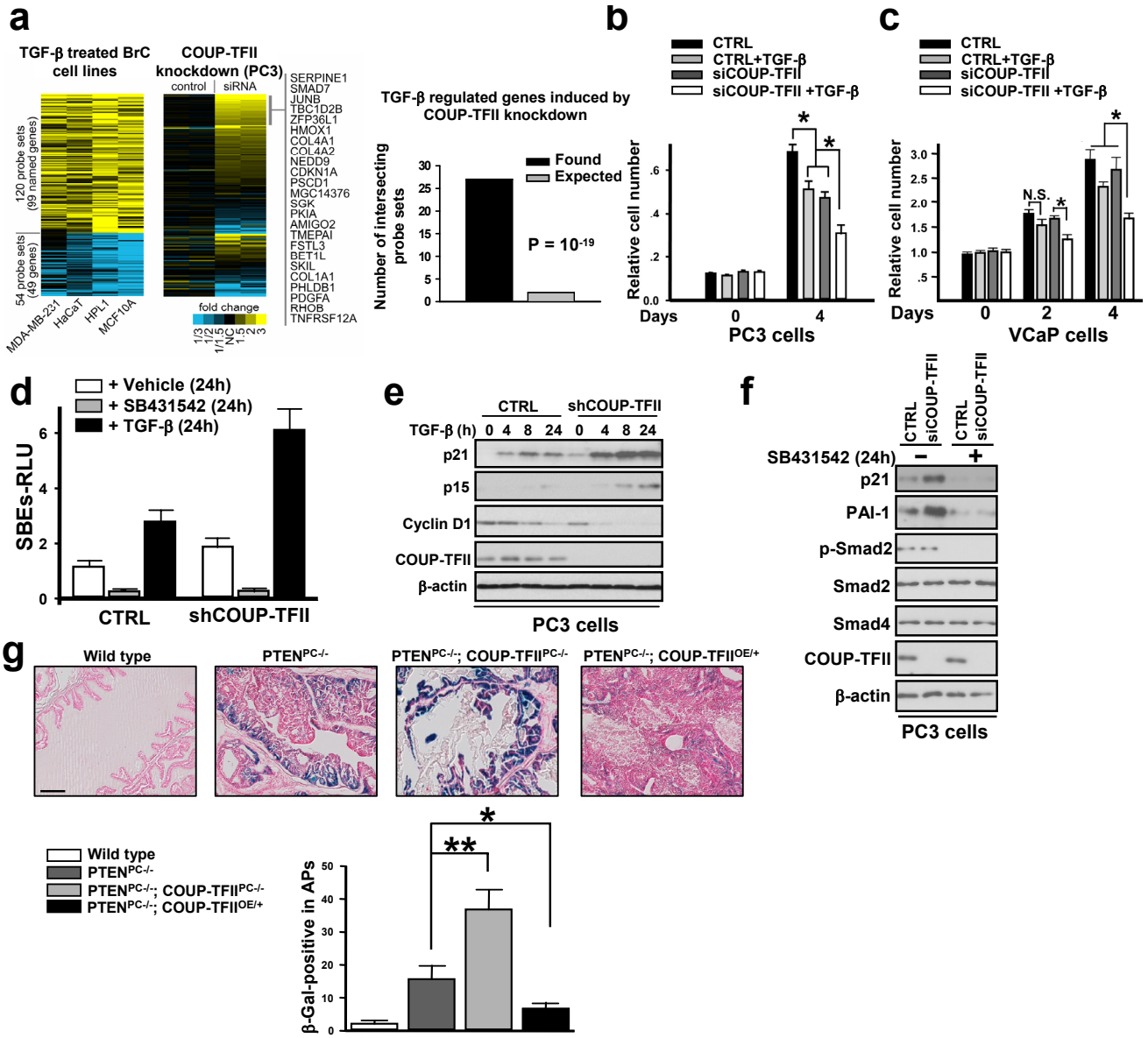

Supplementary Fig. 6. COUP-TFII impacts on TGF-β signaling. (a) Heat map of microarray results shows the enrichment of TGF-β regulated genes in COUP-TFII depleted PC3 cells. The enrichment of TGF-β downstream genes in the absence of COUP-TFII is defined by TGF-β response signature using Fisher's exact test. **(b-c)** Examination of COUP-TFII effects in TGF-β induced growth inhibition in cells. MTT analysis of cell growth in control and COUP-TFII depleted PC3 cells **(b)** and VCaP **(c)** treated with TGF-β. *: $P < 0.05$. Depletion of COUP-TFII renders PC3 (PTEN and AR negative) and VCaP (PTEN and AR positive) cells more sensitive to TGF-β-induced growth inhibition. **(d)** Using a TGF-β-responsive reporter, Smad-binding elements (SBEs)-Luc reporter, we observe a higher TGF-β-induced transcription of SBEs-Luc activity in COUP-TFII knockdown PC3 cells as compared to control cells. In line with this observation, SB43154228, a TGF-β receptor specific inhibitor that effectively abolishes TGF-β signaling, eliminates this enhancement in the same assay **(e)** Western blotting analysis of TGF-β regulated p15, p21 and Cyclin D1 expression in COUP-TFII depleted PC3 cells. **(f)** Western blotting analysis of p21, PAI-1, Smad2/4 and p-Smad2 expression in control and COUP-TFII depleted PC3 cells with or without SB431542 compound treatment. In the absence of TGF-β stimulation, knockdown of COUP-TFII in PC3 cells appears to increase p21 expression. This is likely due to autocrine TGF-β activity in PC3 cells, as SB431542 treatment of COUP-TFII depleted cells completely blocks this increase from the basal level. **(g)** SA-β-galactosidase (β-Gal) staining of 24-week-old APs (N=5). Scale bar, 50 μm. *: $P < 0.05$; **: $P < 0.01$. All the results are obtained from 3 independent repeated experiments. Error bars, Means ± SEM.

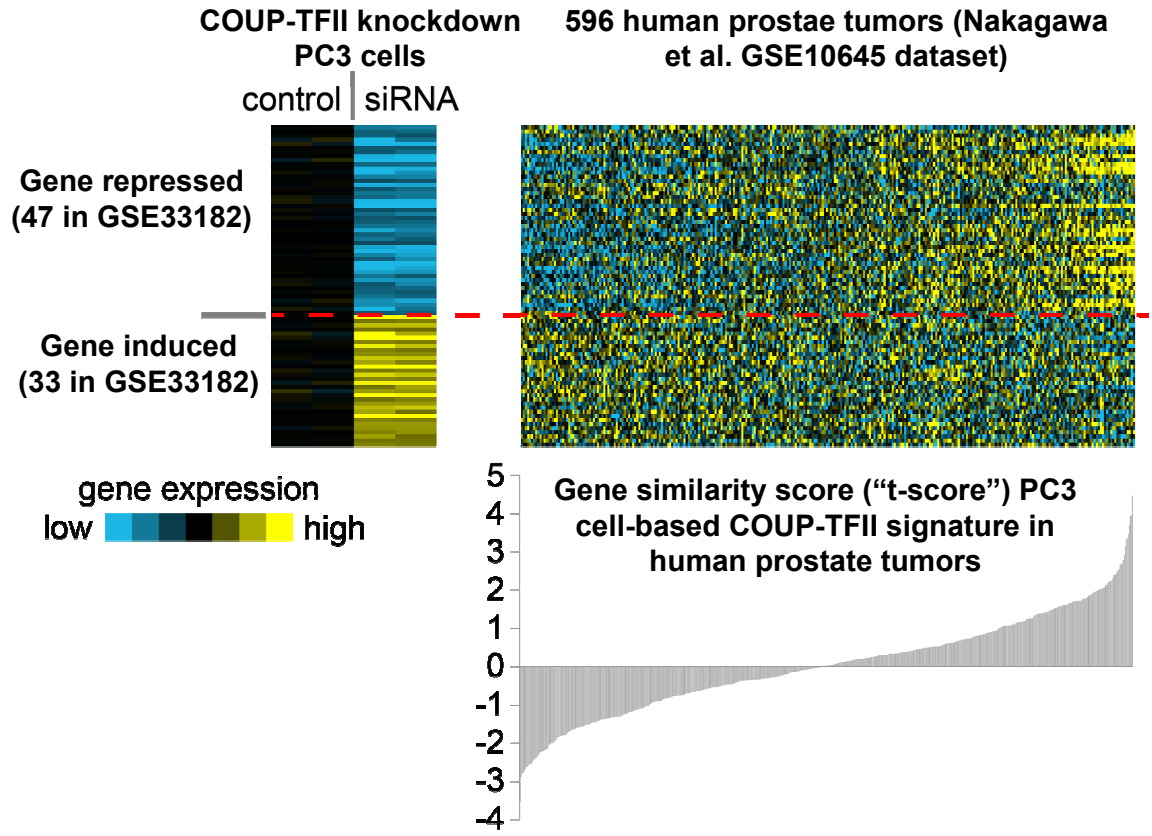

Supplementary Fig. 7. Patterns of the 80 COUP-TFII signature genes that were represented in the GSE10645 dataset of human prostate cancer expression profiles. Below the GSE10645 heat map, a plot of the corresponding t-scores based on COUP-TFII signature is shown. For each human prostate cancer profile, the t-score is computed based on the pre-defined patterns of up-regulation versus down-regulation as observed in the experimental model. For human tumors having a high t-score, genes repressed by COUP-TFII siRNA tend to be high, while genes induced by siRNA tend to be low.

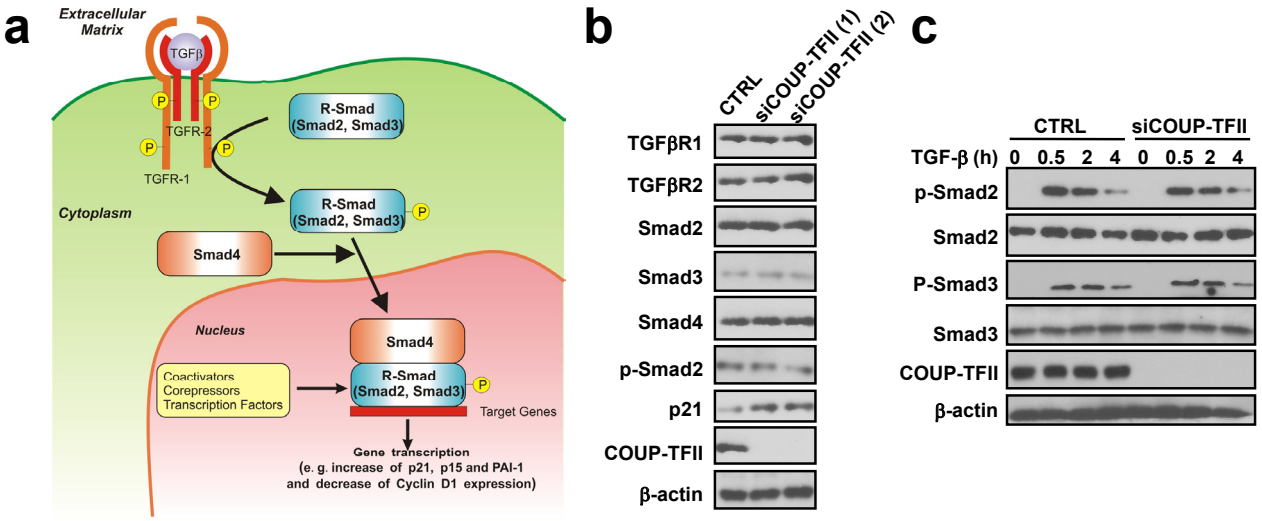

Supplementary Fig. 8. COUP-TFII inhibits TGF-β signaling independent of Smad2/3 activation. To dissect the underlying mechanism for how COUP-TFII represses TGF-β signaling, we investigate whether COUP-TFII regulates the expression of core components that transduce TGF-β signaling, including receptors, receptor-regulated Smads (Smad2 and Smad3) and the common-Smad, Smad4. Depletion of COUP-TFII fails to affect the levels of Smad2/3/4, the receptors or the activated form of p-Smad2/3, suggesting that COUP-TFII acts independent of Smad2/3 activation. **(a)** A scheme of TGF-β signaling pathway. **(b)** Examination of TGFβR1, TGFβR2, Smad2/3/4, p-Smad2 and p21 expression in control and COUP-TFII depleted PC3 cells. **(c)** Control and COUP-TFII knockdown PC3 cells treats with TGF-β and harvests at indicated time points. Cell lysates are subjected to Western blotting analysis using antibodies as indicated.

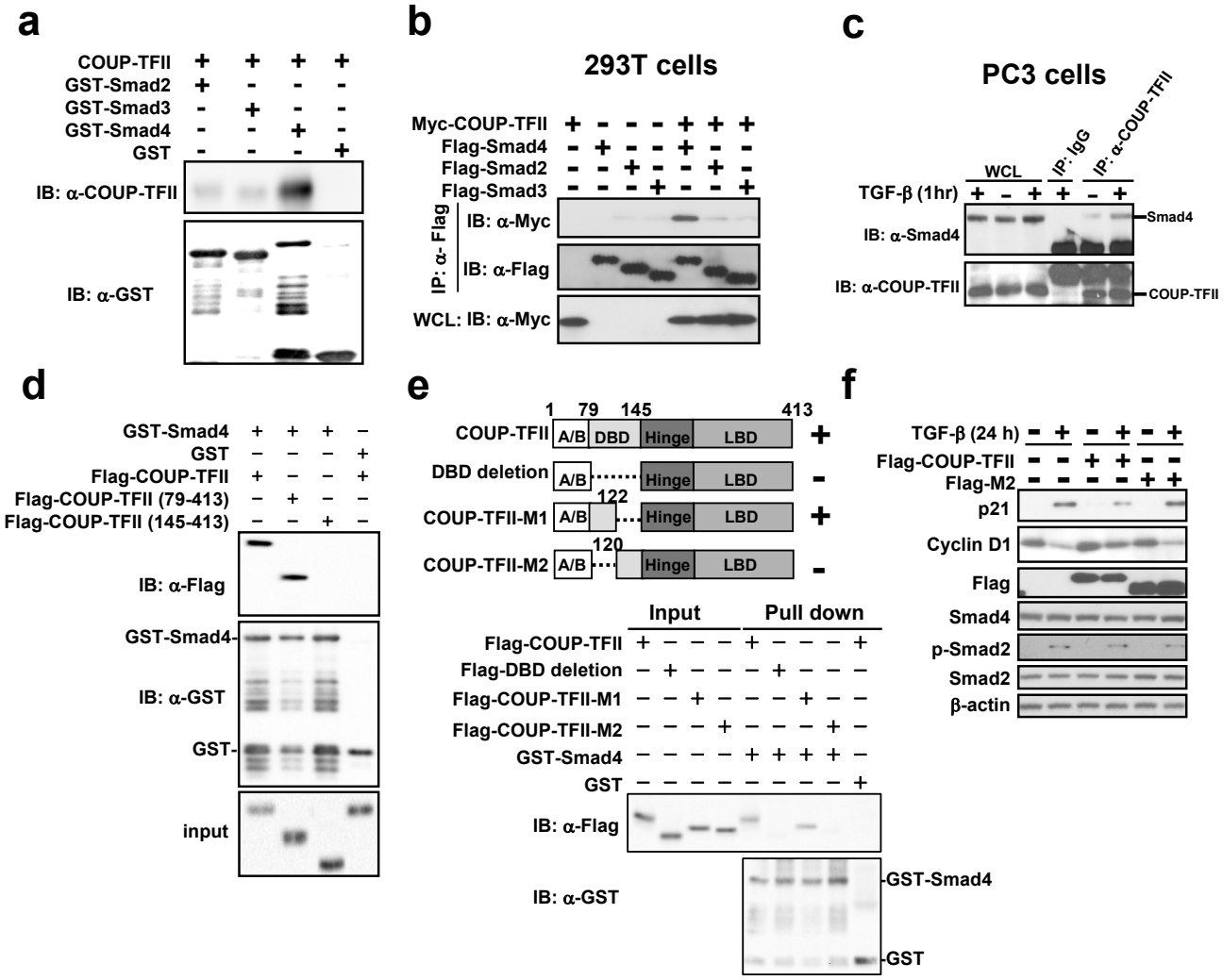

Supplementary Fig. 9. COUP-TFII directly interacts with Smad4. (a) GST Pull-down analysis of the interactions between COUP-TFII and Smad2, Smad3 or Smad4. **(b)** Coimmunoprecipitation (Co-IP) analysis of ectopically expressed Smad2, Smad3, Smad4 and COUP-TFII in 293T cells. WCL: whole cell lysates, IP: Immuno-precipitation. **(c)** Co-IP analysis of endogenous COUP-TFII/Smad4 association in PC3 cells (**(d)** GST-pull down assay indicates that Smad4 interacts with the DBD domain (aa 79-145) of COUP-TFII. **(e)** GST-pull down analysis of the interaction between Smad4 and wild type COUP-TFII, DBD deletion (Δ 79-145 aa), COUP-TFII-M1 (Δ 122-145 aa) and COUP-TFII-M2 (Δ 79-120 aa). **(f)** PC3 cells stably expressing wild type Flag-COUP-TFII or mutant Flag-COUP-TFII-M2, which does not associate with Smad4, are treated with TGF-β and harvest at 24 h. Cell lysates are subjected to Western blotting analysis using antibodies as indicated.

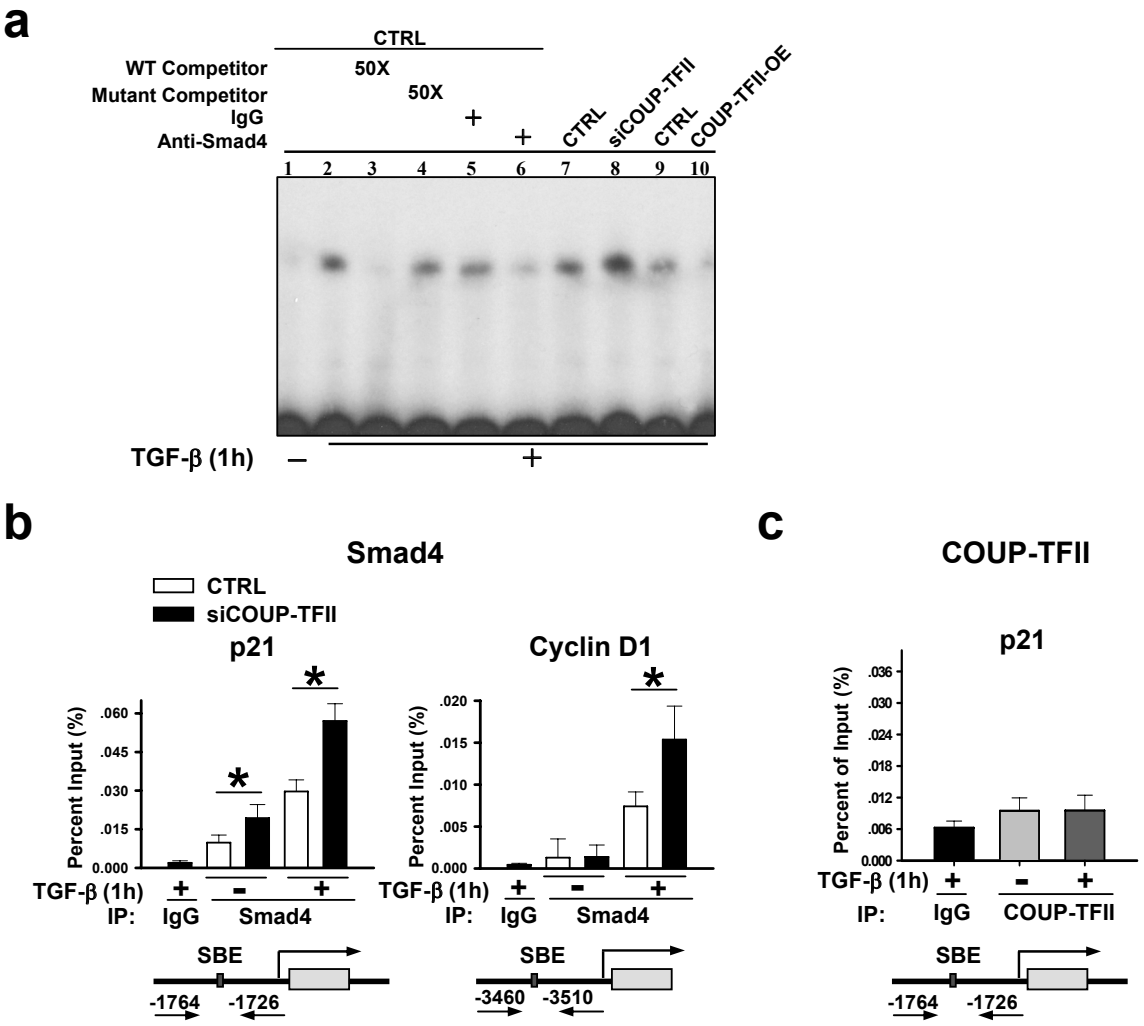

Supplementary Fig. 10. COUP-TFII sequesters Smad4 binding to DNA. (a) Using Gel shift analysis, we notice that down- or up-regulated COUP-TFII increases or reduces, respectively, the binding of Smad4 to its recognizing DNA elements. To validate this observation, we perform ChIP assays to examine the binding of Smad4 or COUP-TFII to p21 and Cyclin D1 promoters. As expected, Smad4 occupies p21 and Cyclin D1 promoter regions containing SBEs in PC3 cells; and these recruitments are further enhanced upon TGF-β treatment **(b)**. However, COUP-TFII does not bind to p21 promoter **(c)**, arguing against an active repressive role of COUP-TFII in p21 regulation. Most importantly, we observe a significant increase of TGF-β induced Smad4 binding to the target gene promoters in the COUP-TFII depleted PC3 cells **(b)**. *: $P < 0.05$; **: $P < 0.01$. The results are obtained from 3 independent repeated experiments. Error bars, Means ± SEM.

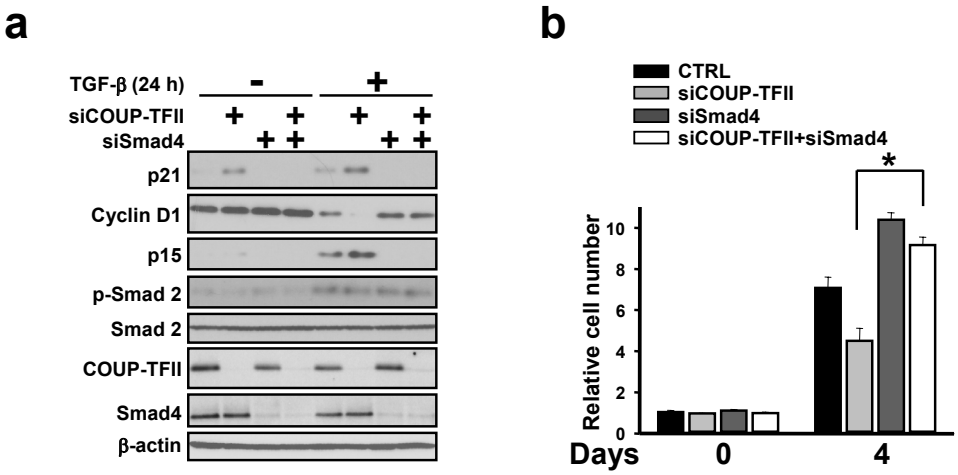

Supplementary Fig. 11. COUP-TFII mediates the growth of prostate cancer cells through regulation of TGF-β signaling. (a) Cell lysates are prepared from control, COUP-TFII, Smad4 and COUP-TFII/Smad4 knockdown PC3 cells with or without TGF-β stimulation, and subjected to Western blotting analysis using antibodies as indicated. **(b)** MTT analysis of cell growth in control, COUP-TFII, Smad4 and COUP-TFII/Smad4 knockdown PC3 cells. *: $P < 0.05$. The results are obtained from 3 independent repeated experiments. Error bars, Means ± SEM.

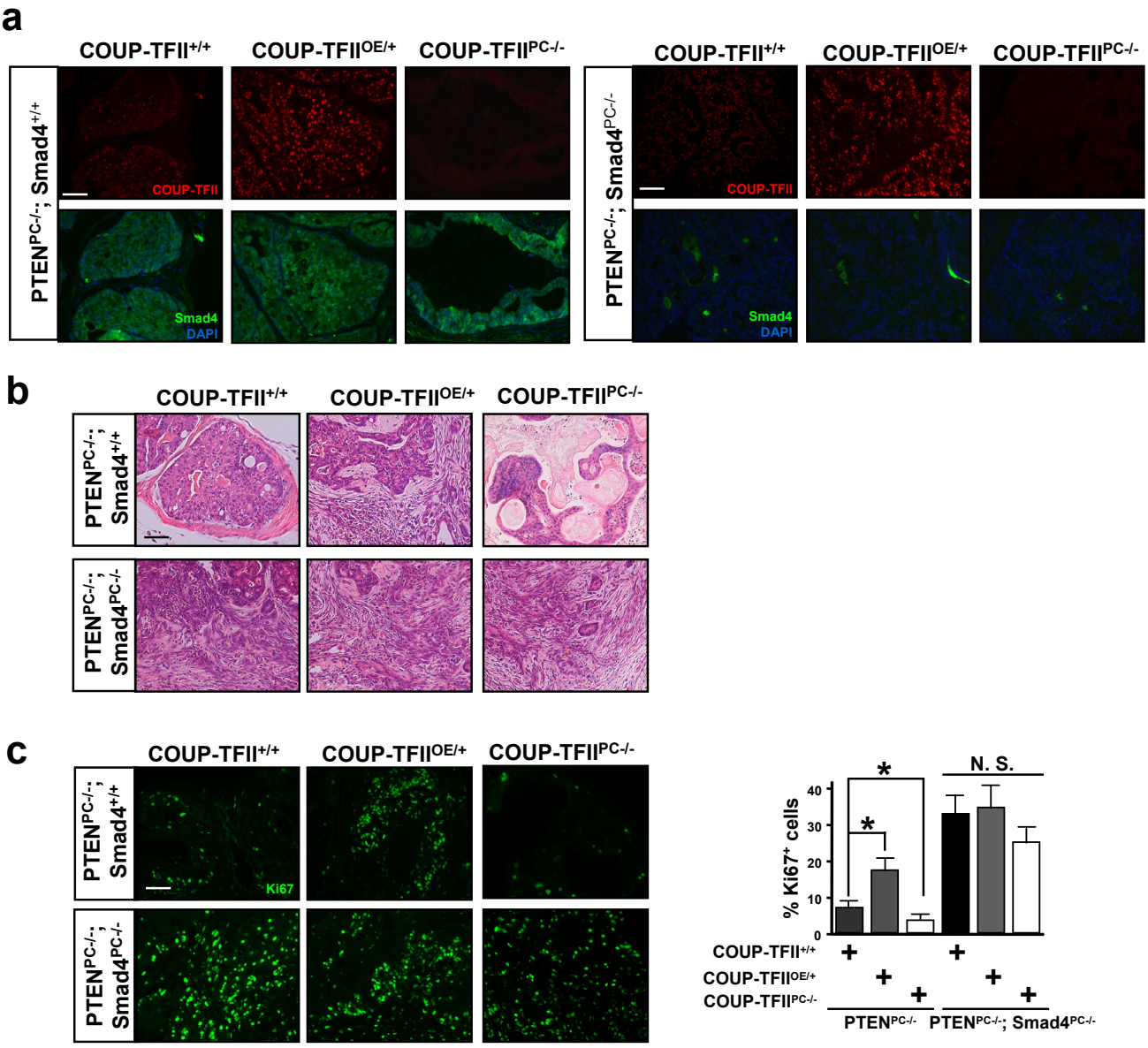

Supplementary Fig. 12. COUP-TFII regulates prostate tumorigenesis in a Smad4-dependent manner. (a) Immunostaining of COUP-TFII and Smad4 expression in prostate epithelium from ($PTEN^{PC-/-}$), ($PTEN^{PC-/-}$; $COUP\text{-}TFII^{OE/+}$), ($PTEN^{PC-/-}$; $COUP\text{-}TFII^{PC-/-}$), ($PTEN^{PC-/-}$; $Smad4^{PC-/-}$), ($PTEN^{PC-/-}$; $COUP\text{-}TFII^{OE/+}$; $Smad4^{PC-/-}$) and ($PTEN^{PC-/-}$; $COUP\text{-}TFII^{PC-/-}$; $Smad4^{PC-/-}$) mice at 5 months of age. **(b)** H&E staining of prostate tumors in a cohort of mice as indicated in the figure at 5 months of age. **(c)** Immunostaining of Ki67 expression in prostate tumors from the entire animal cohort at 5 months of age. The quantitative results of Ki67 staining is shown in right panel (N=6). Error bars, Means ± SEM. Scale bar, 50 μm.

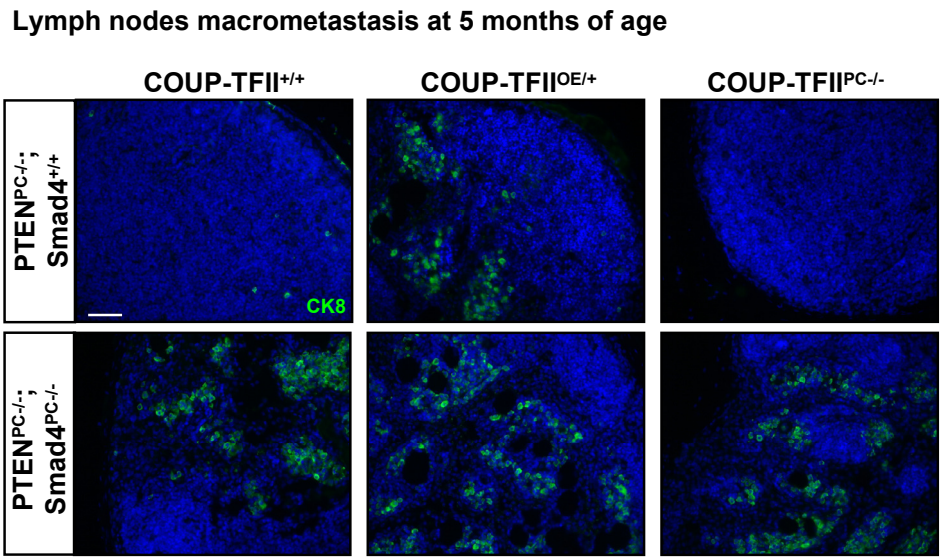

PTEN$^{PC-/-}$	2/10	PTEN$^{PC-/-}$; Smad4 $^{PC-/-}$	10/11
PTEN$^{PC-/-}$; COUP-TFII$^{OE/+}$	8/12	PTEN$^{PC-/-}$; COUP-TFII$^{OE/+}$; Smad4 $^{PC-/-}$	10/10
PTEN$^{PC-/-}$; COUP-TFII$^{PC-/-}$	0/10	PTEN$^{PC-/-}$; COUP-TFII$^{PC-/-}$; Smad4 $^{PC-/-}$	6/9

Supplementary Fig. 13. COUP-TFII promotes prostate tumor metastasis dependent on TGF-β signaling/Smad4. Immunostaining of CK8 expression in lymph nodes from the entire animal cohort as indicated in the figure at 5 months of age. The percentage of mice having lymph node metastasis is shown in the bottom table.

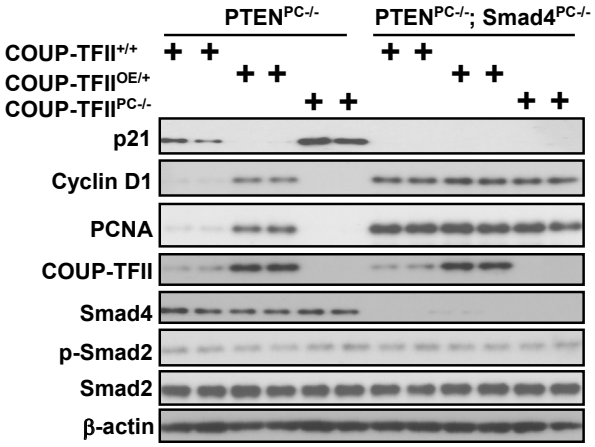

Supplementary Fig. 14. COUP-TFII promotes prostate tumorigenesis dependent on TGF-β signaling/Smad4. Cell lysates are prepared from prostrate tumors in the entire cohort of mice, and subjected to Western blotting analysis using antibodies as indicated. On the molecular level, the comparable levels of p21, Cyclin D1, and PCNA expression between ($PTEN^{PC-/-}$; $Smad4^{PC-/-}$), ($PTEN^{PC-/-}$; $Smad4^{PC-/-}$; $COUP\text{-}TFII^{PC-/-}$) and ($PTEN^{PC-/-}$; $Smad4^{PC-/-}$; $COUP\text{-}TFII^{OE/+}$) mice, argues that COUP-TFII effects in PCa is dependent on TGF-β signaling.

	P-Value	Correlation Coefficient	N
Pre-operative PSA	P < 0.0001	0.235	399
RP Gleason	P = 0.0002	0.24	416
Biopsy Gleason	P = 0.0102	0.126	414
Extracapsular extension	P < 0.0001	0.208	416

Supplementary Table 1. COUP-TFII expression correlates with pathologic variables of PCa aggressiveness. COUP-TFII expressed in tumor cells of PCa patients significantly correlates with pathologic predictors of PCa aggressiveness including PSA levels, Radical Prostatectomy (RP) and Biopsy Gleason Grades, and positive Extracapsular extension. P-values and correlation coefficient are shown in the table.

Supplementary Table 2. COUP-TFII gene signature in prostate cancer

Gene name	Fold changes in COUP-TFII KD PC3 cells	Gene name	Fold changes in COUP-TFII KD PC3 cells	Gene name	Fold changes in COUP-TFII KD PC3 cells
Down-regulated gene list					
BIRC3	0.5326	CDKN2C	0.5311	PML	0.58565
BIRC5	0.3590	CRKL	0.6333	PPP2R1B	0.53741
FAS	0.4522	CSF2	0.2896	PTHLH	0.37341
ARHGDIB	0.5513	E2F1	0.2269	RAD51	0.36112
AXL	0.3643	FANCA	0.4147	SEMA3F	0.60242
BARD1	0.5415	FANCG	0.5489	SPARC	0.22299
BRCA1	0.3960	IGFBP5	0.5698	TK1	0.32970
CCNA2	0.2680	IL1B	0.6043	TOP2A	0.33819
CD44	0.6072	IL6	0.4768	TP53	0.38216
CDC2	0.3020	LIG1	0.5202	TYMS	0.37201
CDC25A	0.3235	IL8	0.2617	DEK	0.55659
CDC25B	0.5849	MCAM	0.5243	ELL	0.56555
CDC25C	0.3923	MYBL2	0.4085	TNFRSF10B	0.56419
CDH11	0.5443	MYC	0.5027	TNFRSF10A	0.46186
CDK6	0.2513	PCNA	0.5324		
Up-regulated gene list					
ARNT	1.66613	IGFBP3	4.1893	PPP2R1B	1.9117
BCL2L1	2.40892	IGFBP5	2.5092	RASA1	1.6041
CBL	1.80718	IL1A	1.8833	JARID1A	1.8842
CBLB	2.30642	ITGB4	1.9612	SH3BP2	1.7136
CCNE1	1.82545	JUNB	3.4222	SKIL	1.7992
p21	2.34575	MLLT6	1.6486	TGFB1	1.7004
COL1A1	1.73425	MMP7	2.5643	VAV2	1.9225
CSPG2	3.30176	MTHFR	1.9830	WEE1	1.8815
EVI1	3.06016	SERPINE1	21.729	YES1	1.76805
FGF5	2.5383	PDGFA	1.7011	FZD7	1.84516
IGF1R	2.2677	PLAT	3.0565		

Supplementary Table 3. Univariate analysis of COUP-TFII gene signature and other genes of interest in PCa-specific death

Univariate Cox	P Value	HR	95% CI
PTEN	0.0017	0.33	0.16 to 0.65
P21	0.032	0.51	0.27 to 0.94
Smad 4	7.97E-07	0.13	0.057 to 0.28
Cyclin D1	0.017	2.6	1.19 to 5.78
COUP-TFII Signature	9.46E-05	1.49	1.22 to 1.81

Supplementary Table 4. Overlap between COUP-TFII siRNA genes and genes correlating with outcome in prostate cancer patients.

Dataset	Gene set	Overlapping Genes	Total genes (P<0.1, Cox)	Enrichment P-value
Genes repressed by COUP-TFII siRNA (891 genes)				
Glinsky	Glinsky_poor_outcome_Recur (P<0.1, Cox)	200	2416	3.5028E-18
Nakagawa	Nakagawa_poor_outcome_Recur (P<0.1, Cox)	20	99	1.5762E-08
Nakagawa	Nakagawa_poor_outcome_DSS (P<0.1, Cox)	20	111	1.1771E-07
Yu	Yu_poor_outcome_Recur (P<0.1, Cox)	63	882	0.00024391
Taylor	Taylor_poor_outcome_Recur (P<0.1, Cox)	85	1297	0.00037813
Taylor	Taylor_good_outcome_Recur (P<0.1, Cox)	98	1560	0.00058492
Nakagawa	Nakagawa_good_outcome_Recur (P<0.1, Cox)	10	93	0.00944193
Nakagawa	Nakagawa_good_outcome_DSS (P<0.1, Cox)	10	113	0.0326385
Yu	Yu_good_outcome_Recur (P<0.1, Cox)	33	571	0.09215239
TGF-beta	TGF-beta_down (P<0.1, Cox)	5	49	0.07012855
Glinsky	Glinsky_good_outcome_Recur (P<0.1, Cox)	90	3030	NS
TGF-beta	TGF-beta_up (P<0.1, Cox)	2	99	NS
Genes induced by COUP-TFII siRNA (829 genes)				
TGF-beta	TGF-beta_up (P<0.1, Cox)	28	99	4.292E-16
Glinsky	Glinsky_poor_outcome_Recur (P<0.1, Cox)	146	2416	3.6603E-06
Yu	Yu_good_outcome_Recur (P<0.1, Cox)	38	571	0.00390359
Glinsky	Glinsky_good_outcome_Recur (P<0.1, Cox)	154	3030	0.00678348
Nakagawa	Nakagawa_poor_outcome_Recur (P<0.1, Cox)	10	99	0.00894999
Taylor	Taylor_good_outcome_Recur (P<0.1, Cox)	83	1560	0.0165403
Yu	Yu_poor_outcome_Recur (P<0.1, Cox)	47	882	0.05953718
Taylor	Taylor_poor_outcome_Recur (P<0.1, Cox)	63	1297	0.13424175
TGF-beta	TGF-beta_down (P<0.1, Cox)	4	49	0.15126068
Nakagawa	Nakagawa_poor_outcome_DSS (P<0.1, Cox)	5	111	0.50552522
Nakagawa	Nakagawa_good_outcome_Recur (P<0.1, Cox)	4	93	0.5560426
Nakagawa	Nakagawa_good_outcome_DSS (P<0.1, Cox)	4	113	NS

Enrichment by one-sided Fisher's exact (using the 19646 genes represented on U133 Plus 2 Affy platform as the total population; NS, not significant). GSE10645 dataset from Nakagawa et al.

Supplementary Table 5. Univariate Cox for COUP-TFII signature score in multiple expression profile datasets of prostate cancer (combined P=0.0005 by Fisher's method).

Dataset	Number of samples	Outcome measure	median follow-up (y)	P-value	HR	95% CI
Nakagawa	596	PCa-specific death	10.7	<0.001	1.49	1.22 to 1.81
Nakagawa	596	Biochemical recurrence	3.6	0.2	1.07	0.97 to 1.18
Glinsky	79	Biochemical recurrence	5.1	0.01	1.55	1.10 to 2.19
Taylor	131	Biochemical recurrence	3.9	0.97	1	0.68 to 1.48
Yu	60	Biochemical recurrence	2.9	0.86	1.04	0.70 to 1.53